Clim. Past Discuss., 6, 537–584, 2010
www.clim-past-discuss.net/6/537/2010/

Climate
of the Past
Discussions

This discussion paper is/has been under review for the journal Climate of the Past (CP).
Please refer to the corresponding final paper in CP if available.

The last glacial maximum locations of summer-green tree refugia using simulations with ECHAM3 T42 uncoupled, ECHAM5 T31 coupled and ECHAM5 T106 uncoupled models

K. Arpe[1,2], S. A. G. Leroy[1], and U. Mikolajewicz[2]

[1]Institute for the Environment, Brunel University, West London, UK
[2]Max Planck Institute for Meteorology, Hamburg, Germany

Received: 16 March 2010 – Accepted: 6 April 2010 – Published: 20 April 2010

Correspondence to: S. A. G. Leroy (suzanne.leroy@brunel.ac.uk)

Published by Copernicus Publications on behalf of the European Geosciences Union.

Abstract

Model simulations of the last glacial maximum (21±2 ka) with the ECHAM3 T42, ECHAM5 T31 coupled and ECHAM5 T106 uncoupled models are compared. The ECHAM5 T106 simulations were forced at the boundaries by results from the coupled ECHAM5-MPIOM atmosphere ocean model while the ECHAM3 T42 model was forced with prescribed sea surface temperatures (SSTs) provided by Climate/Long-Range Investigation, Mapping Prediction project (CLIMAP). The topography, land-sea mask and glacier distribution for the ECHAM5 simulations were taken from the PMIP2 data set while for ECHAM3 they were taken from PMIP1.

The ECHAM5 simulations were run with a variable SST in time simulated by the coupled model. These were also used for the T106 run but corrected for systematic errors. The SSTs in the ECHAM5-MPIOM simulations for the last glacial maximum (LGM) were much warmer in the northern Atlantic than those suggested by CLIMAP or GLAMAP while they were cooler everywhere else. This had a clear effect on the temperatures over Europe, warmer for winters in Western Europe and cooler for Eastern Europe than the simulation with CLIMAP SSTs.

Considerable differences in the general circulation patterns were found in the different simulations. A ridge over Western Europe for the present climate during winter in the 500 hPa height field remains in the ECHAM5 simulations for the LGM, more so in the T106 version, while the ECHAM3 CLIMAP simulation provided a trough. The zonal wind between 30° W and 10° E shows a southward shift of the polar and subtropical jet in the T106 simulation for the LGM and an extremely strong polar jet for the ECHAM3 CLIMAP. The latter can probably be assigned to the much stronger north-south gradient in the CLIMAP SSTs. The southward shift of the polar jet during LGM is supported by observation evidence.

Cyclone tracks in winter represented by high precipitation are characterised over Europe for the present by a main branch from Great Britain to Norway and a secondary branch towards the Mediterranean Sea. For the LGM the different models show very different solutions: the ECHAM3 CLIMAP simulations show just one track going eastward from Great Britain into central Europe, while the ECHAM5 T106 simulation still has two branches but the main one goes to the Mediterranean Sea, with enhanced precipitation in the Levant. This agrees with an observed high stand of the Dead Sea during the LGM. For summer the ECHAM5 T106 simulations provide much more precipitation for the present over Europe than the other simulations thus agreeing with estimates by the Global Precipitation Climatology Project (GPCP). Also during the LGM this model makes Europe less arid than the other simulations.

In many respects the ECHAM5 T106 simulations for the present were more realistic than the ECHAM5 T31 coupled simulation and the older ECHAM3 T42 simulations, when comparing them with the ECMWF reanalysis or the GPCP data. For validating the model data for the LGM, pollen and charcoal analyses were compared with possible summer-green tree growth from model estimates using summer precipitation, minimum winter temperatures and growing degree days (above 5 °C). The ECHAM5 T106 simulations suggest at more sites with findings from pollen or charcoal analyses likely tree growth during the LGM than the other simulations, especially over Western Europe. The clear message especially from the ECHAM5 T106 simulations is that warm-loving summer-green trees could have survived mainly in Spain but also in Greece in agreement with findings of pollen or charcoal.

1 Introduction

Leroy and Arpe (2007), referred to below as LA2007, investigated possible summer-green tree refugia during the LGM using the simulated climate data for the present and the last glacial maximum (LGM). The simulations had been carried out with the ECHAM3 atmospheric model which had a spectral resolution of T42 (corresponds to approx. 2.8° horizontal resolution) and 19 levels in the vertical and was forced with the Sea Surface Temperature (SST) provided by the Climate/Long-Range Investigation, Mapping Prediction project (CLIMAP, 1981). Lorenz et al. (1996) described the set up for these simulations. Model development, however, is an on-going process and the resolution was quite coarse for that investigation; this can be an issue for sites of observed tree refugia in quite topographically structured areas. To improve on their study it was decided to carry out simulations with a more modern model and with a higher spatial resolution.

The SSTs used in the old experiments were provided by CLIMAP (1981) and turned out to be reconstructed only for the Northern Hemisphere while the SSTs differed only slightly from those for the present for the rest of the world, which is hardly realistic. Also, PMIP2 simulations (Braconnot et al., 2007) noted this inconsistency. Therefore coupled ECHAM5-MPIOM atmosphere ocean model simulations were also carried out though with a very low horizontal resolution of T31. These provided the SSTs for an uncoupled ECHAM5 T106 simulation. The ECHAM models including the coupled ocean model were developed at the Max-Planck Institute for Meteorology in Hamburg (MPI).

For a definition of the LGM time we followed Mix et al. (2001) by EPILOG including the maximum extent of the ice sheet. Considering the sea-level constraints and the detailed records of regional climatic change available from the ice cores, the EPILOG group reached a consensus that a preferred LGM chronozone can be defined as the interval between 23 000 and 19 000 calibrated years BP, i.e. 19 500–16 100 ^{14}C years BP. This 4000-yr time window, centred on 21 000 cal. yr BP, encompasses the centre of the LGM event defined previously by CLIMAP (1981), and is long enough to allow the inclusion of much existing palaeoclimatic data in a new synthesis. It is coeval with the lowest stand of sea level (Yokoyama et al., 2000), avoids all known Heinrich Events in the North Atlantic region, and excludes most of Dansgaard-Oeschger climate event 2 (D/O2), as dated in the GISP2 ice core and in the GRIP core with the chronology of Hammer et al. (1997). This definition (21±2 ka) is used here for simulation validation and for deciding if findings of pollen or charcoal from summer-green trees can be assigned to the LGM or not.

The purpose of this study is to show the differences between the different simulations, not only by investigating possible refugia of summer-green trees but also of some basic quantities which should help the better understanding of the final results. To understand the LGM simulation, the simulations for the present climate are needed as well and investigated in detail, as it is only for the present climate that a large amount of data for validation is available. The study is further improved in relation to LA2007 by the inclusion of more sites with observed summer-green tree growth during the LGM, partly from new studies and partly from further literature research.

2 Description of the simulations

The models were run on the one hand with the present-day conditions concerning the orography, solar radiation, ice cover and CO_2. On the other hand the models were run under LGM conditions concerning these parameters (CO_2 – 200 ppm for the ECHAM3 simulation, 185 ppm for the ECHAM5 simulations) as reconstructed by CLIMAP (1981). The high-resolution simulations for the present and the LGM with a T106 resolution (corresponds to approx. 1.125° horizontal resolution) model with 39 vertical levels were carried out with the ECHAM5 atmospheric model (Roeckner et al., 2003, 2006). The boundary data, e.g. the SST and vegetation parameters, were taken from the coupled ECHAM5-MPIOM atmosphere ocean dynamic vegetation model (Mikolajewicz et al., 2007) simulations, which have been carried out for the present and the LGM with a spectral resolution of T31 (corresponding to approx. 3.75°) and 19 vertical levels. The experimental setup is largely consistent with PMIP2. These SSTs were corrected for systematic errors of the coupled run by adding the SST differences between observed SSTs and simulated ones for the present. The largest correction appeared over the central northern Atlantic, halfway between New York and Madrid, providing warmer values up to 8 °C due to a too zonal simulated Gulf Stream. Other areas of large SST corrections are within the Benguela Current reaching St. Helena Island and the Kuro-Shio Current. Otherwise the corrections are generally below 3 °C.

For defining the topography and the land-sea (L-S) mask, the 5 min data sets from PMIP2 (Peltier, 2004) were interpolated linearly to a T106 grid. For deciding on the L-S mask, at the pixel level of 1/12 degree grid, a grid point was called land if the topography was larger than zero. After that the pixels were averaged to the T106 grid. Large lakes were not found by this method. To solve this, a standard L-S mask used at MPI was used to incorporate or correct the following lakes: Caspian Sea, Aral Sea, Lake Baikal, some smaller lakes in northern Russia, Lake Vaenern in Sweden, the Great Lakes and some further lakes in Canada, Lake Chad, Lake Victoria and a widening of the Congo River creating one grid point regarded as a lake. On the other hand, some smaller fjords on the Greenland coast were assumed to be land. Lake Eyre in Australia is, according to the 0-orography criterion, a lake but as it is mostly dry it was assumed to be land. The same criteria have been used for the LGM data set and the resulting L-S mask was compared with the present-day L-S mask just created. For some northern lakes, the glacier mask utilized over-ruled the question of lake or no lake, e.g. for the Great Lakes. The provided data set did not have a Caspian Sea although large parts of it are deeper than −100 m. A controversial discussion about the size of the Caspian Sea and the Black Sea during LGM is still going on. For the Black Sea we took the shape as provided by the PMIP2 data using the zero-level criterion. For the Caspian Sea it is known that there was a Caspian Sea during LGM. However, it is not known whether it was larger (because of possible diversion of northward flowing rivers to the south due to glaciers along the Arctic coast), or smaller (because of a possible dryer climate) and therefore, for the LGM simulation, we left it as it is now. The same decision was taken for other lakes. Also Lake Eyre was assumed to be dry during LGM.

The coupled ECHAM5-MPIOM atmosphere ocean dynamic vegetation model (Mikolajewicz et al., 2007) also provided the vegetation parameters for the T106 model. Along the Arctic coast of western Siberia, the glacier data and the land using the 0-orography criterion left a gap which would create two large lakes into which the Ob and Yenisey Rivers would discharge. The glaciers north of it would prevent drainage into the ocean and larger lakes would evolve, which Grosswald called Pur and Mansi Lakes

(Grosswald, 1980). Using the PMIP2 data, the water level of these lakes would need to rise at least 170 m before the water could drain into the ocean. This level is used in this study to define such lakes.

The interpolation from the T31 resolution of the coupled model simulation to T106, needed for forcing the uncoupled run, was done linearly. Some grid points, however, needed special consideration because of the large difference in resolution which allowed large differences in topographic heights and had a more structured L-S mask in the T106 resolution.

As a criterion for selecting a suitable 25 year period from the 1500 years of simulation with the coupled model, we decided to use a period of lowest SST variability to avoid extremes.

3 Differences between the simulations

3.1 SST

Figure 1 shows annual mean SST differences between LGM and the present (NOW) using different estimates. ECHAM5 T106 is the one extracted from the ECHAM5-MPIOM coupled model (in this presentation both should be identical and therefore are marked here as ECHAM5) and used in the present simulations. CLIMAP (1981) and GLAMAP (Sarnthein et al., 2003) are estimates used in the PMIP1 simulations. The differences are obvious. CLIMAP provides the coldest LGM temperatures for the North Atlantic and ECHAM5 the warmest. For the remaining oceans ECHAM5 has the coldest temperatures while the other two have even warmer temperatures in places during LGM than NOW (light shading), which seems unrealistic. Some areas in the summer hemisphere (not shown) appear much warmer during LGM than NOW. These are areas which were continents during LGM while they are oceans now, such as along the NE coast of Siberia or the SE coast of Argentina. For the North Atlantic more cooling in the Arctic than in the tropics means a stronger north-south SST gradient during LGM than NOW in all simulations, especially in CLIMAP.

The differences between CLIMAP and the ECHAM5 simulation in the SSTs are in agreement with PMIP2 (Braconnot et al., 2007). Otto-Bliesner et al. (2009) further suggest that these new simulations are in general agreement with new tropical SSTs reconstructions from the MARGO project (Kucera et al., 2005). The PMIP2 models give a range of tropical (defined as 15° S–15° N) SST cooling of 1.0–2.4 °C, comparable to the MARGO estimate of annual cooling of 1.7±1 °C. This fits well with the ECHAM5 simulations, shown in Fig. 1. The PMIP2 models simulate greater SST cooling in the tropical Atlantic than in the tropical Pacific, while the ECHAM5 simulations suggest more cooling for the tropical Pacific.

The consequences of the SSTs for the temperatures over Europe during winter and summer are shown in Fig. 2 where the 2 m temperatures (2 mT), as simulated for the present (NOW) and LGM and as observed using ECMWF reanalysis data (OBS), are displayed. Comparing the 2 m temperatures of the simulations for the present shows clearly the best performance of the T106 model, e.g. over Western Europe. The differences between the two ECHAM5 simulations are not only due to the different resolutions but also due to differences in the SSTs, as the T106 SSTs are corrected for a systematic error of the coupled model, as explained above. The up to 8 °C cooler SSTs over the North Atlantic in the coupled simulations may have led to some cooler 2 mT over Europe compared with the T106 run for the present and LGM. In winter the cooler North Atlantic SSTs during LGM in the CLIMAP data generate clearly cooler 2 m temperatures for Western Europe while the two ECHAM5 simulations provide cooler temperatures for Eastern Europe. A standard Atmospheric Model Intercomparison Project (AMIP – Gates, 1992) type simulation data set with different resolutions is available at MPI (CERA, 2010, see also Arpe et al., 2004). In these data sets the different atmospheric models were driven by the same external forcings including monthly mean observed SSTs. From these the sole impact of resolution can be found and indeed the T106 and coupled simulations would look more similar without the SST corrections in the T106 run. The CLIMAP simulation for the LGM has much more zonally orientated isotherms and has a very strong gradient over the Atlantic which probably has an impact on the general circulation.

Note the much more structured cooling over the Alps for summer in the T106 simulation during LGM compared to the other runs shown in Fig. 2b. This turns out to become important in the discussions below.

The CLIMAP run for the LGM provides clearly lower temperatures in summer for most of Europe north of 45° N (the latitude circle in Fig. 2b) compared with the other runs.

3.2 Height field at 500 hPa

Figure 3 shows the 500 hPa height fields for the present, overlaid in thinner lines with grey shading, which show the difference between LGM and the present. Darker grey shadings indicate that during the LGM the 500 hPa height field was lower than NOW, e.g. for T106 during winter the Alaskan ridge and the trough over eastern US were much stronger during the LGM. The coupled model shows similar patterns while the simulation with CLIMAP SSTs is very different: the ridge over Western Europe shown for the present is completely wiped out for the LGM.

For summer the changes from NOW to LGM are less pronounced in all simulations. A slight ridging over Eastern Europe during LGM might be of importance.

3.3 Upper air wind

In Fig. 4a, the zonal wind for winter (DJF), which averaged between 30° W and 10° E, is shown. The upper panel is the observation as produced by the ECMWF re-analysis (ERA40, Uppala et al., 2005). The lower two panels show the wind as simulated by the T106 model for the present and the LGM; overlaid in thinner lines and highlighted by grey shading are the differences from the field in the panel above, i.e. the shadings in the middle panel show the model error for the present and in the lower panel they show the change between the LGM and the present as simulated by the same model. The

T106 simulation for the present has a subtropical jet (20° N, 200 hPa) which is slightly too weak and stretches too far to the south. The polar jet (50° N, 300 hPa) is slightly stronger than analysed.

During LGM the polar jet is even stronger and 7° further south while a reduction in the westerlies occurs at 60° N suggesting that the polar jet is forced by the massive ice sheet to go either further south or north of it. This fits in with enhanced precipitation over the Mediterranean during LGM, shown below. The stronger jet fits in as well with the stronger north-south gradient of surface temperatures shown in Fig. 1. Florineth and Schlüchter (2000) suggest from palaeo-data a more southerly position of the main flow during LGM over the Alps, supporting the simulation by the T106 model.

Figure 4b shows the same presentation for the coupled model and the older CLIMAP simulations. The T31 resolution of the coupled run is not sufficient for getting the dynamics of the atmosphere completely right and therefore one finds here the largest differences between the simulations for NOW and the observation, indicated by the shading in the top panel, presenting the difference between the coupled simulations for the present and observations. This model hardly shows a separation between the polar and the subtropical jet. The difference between the LGM and present-day simulation bears, however, some similarities to those of the T106 simulations. The changes from the present to LGM are strongest in the CLIMAP simulations. The polar jet (50° N, 300 hPa) was already enhanced in the T106 run for LGM by more than 4 $\mathrm{m\,s^{-1}}$ compared with the present but in the CLIMAP simulation the increase is more than 30 $\mathrm{m\,s^{-1}}$, probably due to the much colder SSTs in the northern Atlantic and warmer tropical SSTs during LGM in the CLIMAP data compared to the ECHAM5 simulations. Such a stronger north-south SST gradient provides a stronger forcing for the atmospheric circulation

3.4 Surface winds

LA2007 noticed a massive increase of winter surface wind in the CLIMAP simulations for LGM over Europe. This can also be seen in the cross-sections of the zonal mean wind at 1000 hPa shown above (Fig. 4) with increases of 5 m s^{-1}. In this presentation at this level the difference in wind speed for the other simulations was very small. Maps of summer and winter mean surface winds (not shown) demonstrate as well a much lesser increase in wind during winter LGM for the two ECHAM5 simulations. Common to all simulations is an increase in the trade winds off North Africa in summer and an increase in the North Atlantic westerlies in winter for the LGM.

3.5 Precipitation

Figure 5a, shows the winter (DJF) simulated precipitation for the present (NOW) and the LGM. Also the estimate by GPCP (Huffmann et al., 1996) using observations is included. All simulations for the present show similar features to those observed. One can, however, easily see that the T106 simulation fits best to the observations. For the LGM LA2007 have previously pointed out that the cyclone tracks, indicated by the precipitation patterns, take a very different course in the LGM simulations compared with the present, i.e. during LGM the cyclones in the CLIMAP simulations move straight eastward into Europe instead of towards Scandinavia as for the present. In the T106 simulations a branch towards Scandinavia can still be seen for the present as well for LGM though weaker for the LGM and a second branch towards the Mediterranean, somewhat stronger during LGM reaching Lebanon/Israel/Jordan. This branch is clearly further south than in the LGM CLIMAP simulation. The T106 simulation with higher precipitation in the Levant is probably realistic as it is known that the Dead Sea had a high stand during LGM (Stein et al., 2009). The shift of the precipitation towards the Mediterranean Sea during the LGM also fits the study by Florineth and Schlüchter (2000) who found that the precipitation for the Alpine glaciers had their source to the south of them.

During summer (JJA) for the present (NOW), shown in Fig. 5b, the lower resolution model simulations show less precipitation over the northern Atlantic and northern Europe than the observations while the T106 model seems to be most realistic.

Comparing the LGM simulations with those for the present, one finds much less aridity for LGM in the ECHAM5 simulations (T106 and coupled) for Europe than in the CLIMAP simulations, probably due to the much warmer northern Atlantic SSTs in the ECHAM5 simulations. Over Western Europe, the T106 simulation provides even more precipitation for LGM compared with the present.

The differences between the T106 and the coupled runs are not only due to the different resolutions but could also be influenced by the warmer SSTs in the T106 simulations as they had been corrected by the systematic error of the coupled run, as described above. A standard AMIP type simulation data set with different resolutions is available at MPI (CERA, 2010) from which the sole impact of resolution can be identified (Arpe et al., 2005). Indeed the T106 and coupled simulations would look more similar without the SST corrections in the T106 run.

These changes in the precipitation over Europe are consistent with the changes in the upper air wind field discussed above.

Braconnot et al. (2007) compared the precipitation in the PMIP2 coupled model simulations with the uncoupled PMIP1 simulations and found less drying for central and southern Europe in the PMIP2 coupled simulations, even with an increase of precipitation for Western Europe during the LGM in annual means. In annual means for Western Europe the ECHAM5 T106 simulations also provide an increase in precipitation during LGM of up to 90 mm season^{-1} (not shown) which is similar to the PMIP2 results. The coupled ECHAM5 simulations have an increase of only a third of the T106 values.

It is remarkable that hardly any change occurs between NOW and LGM over the Himalayas both in summer and winter in all simulations, which might be important for river discharge into the Aral Sea (not shown).

3.6 Precipitation minus evaporation

The availability of water for run off and vegetation is best been shown by the difference between precipitation and evaporation (P-E). In Fig. 6 annual mean differences between LGM and NOW are shown. Because of model constraints, P-E has to be positive over land because only water which has fallen can be evaporated. For the lower resolution simulations, some negative numbers along coasts can occur over continents due to interpolations to T106 for plotting which result in Fig. 6 in less strong gradients along coastal lines. Above, a general reduction of precipitation for the LGM is shown which is not reflected in the P-E plots as the evaporation is also reduced during LGM. Over Western Europe including the Iberian Peninsula P-E is even enhanced in all simulations especially for T106. For Lebanon and Israel in the T106 run an enhanced availability of water for LGM is clearly indicated (for the coupled runs only slightly), in accordance with an observed higher stand of the Dead Sea. The ECHAM5 simulations show less water availability during LGM for Eastern Europe. If one is interested in intra- or inter-annual variability the best variable to look at would be the soil-moisture but its calculation depends on many less well-known quantities.

Of special concern has been the water budget of the Black, Aral and Caspian Seas. Averages of P-E for the basins of these three seas/lakes suggest that hardly any change occurs between NOW and LGM for the Black Sea, with some decline in the water supply for the Caspian and Aral Seas. For the three lakes/seas the evaporation has similar values for the present as that provided by the ECMWF re-analysis (ERA40, Uppala et al., 2005), while for the LGM the evaporation drops by about a third. The amounts of precipitation drop, however, even more, with the least drop for the Black Sea.

These results suggest that the Caspian and Aral Sea should have had a lower level than today and the Black Sea a similar level, unless there has been a diversion of the north-ward flowing rivers due to the blockage by glaciers. The model does not have any constraint concerning the water budget over lakes and seas, while over land the precipitation has to be larger or equal to the evaporation, therefore no absolute figure can be given.

4 Possible summer-green tree growth during LGM

So far it has been shown in many examples that the ECHAM5 T106 simulation provides the best reproduction of the present climate. Intuitively one may assume that the model which provides best estimates for the present climate would also be best for simulating a climate with a different external forcing such as during the LGM. Validation is, however, difficult but some aspects have already been discussed above where the T106 simulation seems to be more realistic, e.g. the more southerly position of the cyclone track over the Mediterranean Sea into the Levant, explaining the high stand of the Dead Sea during LGM, and a southward shift of the polar jet. We use here the method from LA2007 to estimate the likeliness of summer-green tree growth during the LGM and compare this with the available pollen and charcoal findings. There, and in this study, a simple down-scale method is used which partly compensates for systematic errors. For this down-scaling the difference between the simulations for LGM and for the present is added to a high-resolution climatology (Leemans and Cramer, 1991) of the present.

A better model should give possible tree growth at more sites with verified growth. Warm-loving and cold-tolerant summer-green trees are investigated. Typical warm-loving trees in this investigation are: *Castanea, Juglans, Platanus, Rhamnus, Fraxinus ornus, Vitis, Quercus pubescens* and *Ostrya*, and cold-tolerant trees are: *Carpinus, Corylus, Fagus, Tilia, Frangula, Acer, Populus, Fraxinus excelsior, Alnus, Quercus robur* and *Ulmus*. More details can be found in LA2007.

A few sites have been suggested by scientists as possible refugia for trees during LGM; but those sites without a proof or where the observations were not properly dated or did not cover the LGM, were not included in our study. Reliable sites had to have a sub-continuous curve of at least one taxon from our list and an age of 21±2 cal. ka. A few marine sites which fulfil the requirements are also given in Table 1. However, it is often not clear where the pollen found at those sites came from, either by river or wind transport, e.g. off the coast of Portugal. Because of the large source area for the pollen, the number of potential grid points needs to be increased. Only little weight was given to these sites in our investigation. All the sites are listed in Table 1.

At the sites 7, 18, 19 and 34 some pollen occurrences of warm-loving trees have been found but do not have the required sub-continuous curve of at least one taxon. Nevertheless we kept them as sites with warm-loving trees, especially the ones for Greece because there are three nearby sites of the same quality which suggest at least one refugium in the area. For Siles (site 7) the pollen might have been transported from the other nearby sites with warm-loving trees and its inclusion in or absence from our list hardly affects the conclusion of the study.

LA2007 used the summer precipitation, the minimum monthly mean 2 m temperature and the growing degree days (above 5 °C) (GDD5) as limiting factors for possible tree growth. Similarly, for each of these variables and the combined score the possible tree growth in the three simulations is investigated.

4.1 Precipitation

Figure 7 shows the precipitation for JJA after a simple downscaling to a 0.5° grid (see LA2007). The much stronger precipitation over western and central Europe in the T106 simulation, especially compared to CLIMAP, has already been shown above. Most observation sites lie in areas with grey shading (meaning more than 50 mm precipitation per season) which is sufficient for possible growth of cold-tolerant trees. Warm-loving trees have a requirement of 60 mm season^{-1} which is hardly any different from the 50 mm season^{-1} in the plots. Sites 21, 22 and 23 in Table 1, the easternmost continental sites, lie in areas which have deficient summer precipitation in all three simulations. Sites 22 (Ghab) and 23 (Urmia) are in areas devoid of summer precipitation in the present climate. The two southern marine sites off Portugal are quite distant from land with sufficient precipitation for tree growth.

A more detailed investigation, however, (see Tables 2 to 4) shows that Gibraltar also has too little precipitation when using the nearest grid point, probably because a 0.5° grid is too coarse for capturing the rough topography of this peninsula. One has to look into the surrounding 1.5° away to find a grid point with sufficient precipitation. The T106 simulation provides most precipitation for the grid point nearest to Gibraltar. The same argument probably applies as well for site 20, a small Greek island along the Turkish coast, though even at 1.5° away not enough precipitation can be found; again T106 provides most.

Sites 4 to 6 in southern Spain have borderline values in the T106 simulation but one has to look only for neighbouring grid points half a degree away, e.g. in the Sierra Nevada, to find sufficient precipitation and one would hardly call the simulations a failure for these sites. The same applies for sites 18 and 19 in Greece for warm-loving trees. In the CLIMAP runs, these sites have extremely low values at the nearest grid point, even sometimes with negative values which can happen when the change from NOW to LGM in the simulations is larger than the observed precipitation at that point.

It has been shown above that the T106 model produced a much wetter Western Europe than the other models, even wetter than for the present, and the question is whether that is more or less realistic. The first 10 sites in Table 1 are from Spain and are affected by the precipitation differences. T106 comes closest to reach at least 50 mm season^{-1} for all the sites concerned and gives the best results while CLIMAP the worst. For sites 3 and 6 in southern Spain the difference between the present and LGM in the CLIMAP simulation was even larger than the observed precipitation leading to negative precipitation values for the CLIMAP run due to the down-scaling method used here. So the wetter Iberian Peninsula in T106 is supported by findings of summer-green trees during the LGM.

A similar trend can also be found for sites 18–23. Site 23, Urmia, is a lake in a very arid area in north-western Iran. Lake Urmia (or Orumiyeh), is one of the largest permanent hypersaline lakes in the world and resembles the Great Salt Lake in the western USA in many aspects of its morphology, chemistry and sediments (Kelts and Shahrabi, 1986). No tree growth can be found in its surrounding area now. Figure 6 suggests only small changes in available water between NOW and LGM, in fact a small decrease in annual mean available water (P-E) can be found in the T106 and

CLIMAP simulations. Therefore one has to assume that the pollen found there have been transported from further away. The prevailing wind in the ERA40 observation data in May to July, using monthly mean zonal and meridional wind components, is from the east with low wind speeds. This wind is best simulated by the T106 model for the present though with some increase of speed and a slightly more northerly component. The simulation for LGM hardly differs in this respect from the present, so the source of pollen at Lake Urmia is the coastal area of the Caspian Sea.

Site 22 in Syria is also a very dry area in summer though with sufficient precipitation in spring and winter. Figure 6 suggests some more available water in annual means during the LGM. At the present time the trees under consideration here could only survive along rivers and it is doubtful that it was much different during the LGM.

Sites 18–20 in Greece are at the borderline concerning precipitation for warm-loving trees in the ECHAM5 simulations, i.e. near 60 mm season^{-1}, while they are much dryer in the CLIMAP simulations, providing evidence for the superiority of the more recent model.

4.2 Temperature of coldest month

A further limiting factor for summer-green tree growth is the minimum monthly mean temperature. Earlier it has been shown that the CLIMAP simulation is quite different in this respect, cooler in Western and warmer in Eastern Europe, compared with the two ECHAM5 simulations, probably due to its much colder North Atlantic. This can be seen in Fig. 8, the down-scaled presentation, as well as in Fig. 5b, especially over Eastern Europe and Turkey. The higher model resolution T106 leads to warmer temperatures for Iberia and NW Africa in the ECHAM5 simulations. Earlier, a standard AMIP type simulation data set with different resolutions (CERA, 2010) has been used to highlight the sole impact of resolution. Again these experiments suggest that the difference between the two runs is due to the warmer SSTs in the North Atlantic in the T106 simulation. For most of Iberia one finds observation sites in the lightly shaded areas ($> -2.5\,^{\circ}$C) more so in the T106 simulation, i.e. areas with possible growth of warm-loving trees. The exception is at the grid point of site 9 (Spanish Pyrenees) but only cold-tolerant trees have been found there. The same applies for the CLIMAP simulations at sites 3, 8 and 9. The minimum temperature does not suggest superiority for any of the simulations for Western Europe.

Two sites in the Po Valley (sites 11 and 12) fail on this criterion for the warm-loving trees in all simulations, with the worst in the T106 simulation (−9 versus −5 °C). Neither site reports the existence of warm-loving trees, however, a nearby coring in the Venice Lagoon (Canali et al., 2007) shows findings of *Ostrya*, a warm-loving tree, and cores covering the LGM in the Venetian Po Plain show poorly documented occurrences of *Castanea* sativa type (Miola et al., 2006). These sites have not been included in our list of reliable sites because of various uncertainties. In Fig. 2a it could be seen that the winter temperature difference between NOW and LGM is much more pronounced over the Alps in the T106 simulation compared with the others. This can be assigned to the different representation of the Alps and the Adriatic Sea in the different resolutions of the models. LA2007 showed a better representation of the Alps in a T106 model though with a southward shift of the Po Valley while the other resolutions did not have a Po Valley at all. This creates a much warmer (more realistic) temperature for the present in the T106 simulation than in the lower resolution models. As the down-scaling method uses only the difference between LGM and NOW from the simulation, it results in cooler temperatures for the LGM in Fig. 8 for the Po Valley.

At the grid points of the two sites 14 and 16 in Austria and Slovakia, only the T106 simulation has values below −15 °C (less cold in the other two simulations), which does not agree with the findings of trees there, though the other simulations fail at these stations because of the growing degree days criterion (see below). The largest differences between the models are at site 16 with temperatures of −18.2 (T106) versus −13.5 °C (CLIMAP). Perhaps these sites lie in areas with a local climate which is not resolved by the present data and a higher resolution climatology model might alter this finding. Using the Peltier (2004) orographic data on a 5 min grid, one finds a variation between minimum and maximum height on a 1 degree grid from 127 to 1308 m, though the mean for a 0.5 degree grid, the one used for the climatology (Leemans and Cramer, 1991), here has a height of 555 m near to the one at the site of pollen findings during LGM. A range of heights of 127 to 1318 m corresponds to a temperature range of 8.8 °C when applying a standard atmospheric lapse rate.

At several sites across Europe, Peyron et al. (1998) estimated the coldest mean temperature and annual mean precipitation by grouping pollen taxa into plant functional types (PFTs). These reflect the vegetation in terms of biomes which have a wider distribution than a species. For the present-day, one can provide a range of minimum temperatures and precipitation in which such PFTs can grow. As the same PFTs can also be found during the LGM, it allows the estimation of ranges of minimum temperatures and precipitation during LGM. Some of their sites are the same as those used in this study, i.e. sites 5, 15, 18, 19 and 22 (Table 1). At these sites the minimum temperatures given in this study are much warmer than those suggested by Peyron et al. (1998). This suggests for the two Greek sites (18 and 19) that warm-loving trees could not have grown according to the PFT method although some pollen grains have been found there. They also provide annual mean precipitation estimates at these sites which are much lower than those provided by all three model simulations (not shown). We did not follow up this comparison any further.

On the whole it cannot be judged from the available data, whether the large-scale differences in the patterns of the minimum temperature are more realistic in the one or the other simulation.

4.3 Growing degree days

The growing degree days above 5 °C (GDD5) is a less strong limiting factor for tree growth than precipitation. Only a few sites are in or near areas with values <800, needed for the growth of cold-tolerant trees, i.e. sites 9 in the Pyrenees, 14 in Austria and 16 in Slovakia of which in T106 sites 14 and 16 failed on the minimum temperature (Fig. 9). In the other two simulations, these sites also failed on this criterion. Further sites in the coupled run (7, 8, 15 and 17) failed at this criterion as well. For most of these sites sufficient GDD5 values are reached only one grid point away from the site, so it might only be a resolution problem. Only Duttendorf in Austria and Safarka in Slovakia (sites 14 and 16) fail on this criterion in the CLIMAP run and only Duttendorf in T106 also for ±0.5°.

Warm-loving trees need at least 1000 GGD5 which is easily surpassed at all sites with findings of warm-loving trees.

4.4 Temperature of the warmest month

A further limiting factor is the temperature of the warmest month which has to be higher than 12 °C, according to van Campo (1984). This limit has not been included in the combined scoring factor for possible tree growth below, as in all cases where the 12 °C criterion was not met also the GGD5 criterion was already a limiting factor.

4.5 Summary for summer-green tree growth during the LGM

Possible growth of summer-green trees is found in a belt between cold temperatures in the north and too low summer precipitation in the south. The topographic impact can clearly be seen as mountains are often connected with enhanced precipitation but also with reduced temperatures. As the limits given by the precipitation are similar for warm and cold-tolerant trees, i.e. 50 mm for cold-tolerant and 60 mm for warm-loving trees, the southern limits for both sorts of trees are very similar. The GDD5 and the minimum temperatures are somewhat complementary but slightly more sites fail on the growing degree days criterion.

In Fig. 10, all limiting factors are taken together. In grey shaded areas (values >1) at least the minimum requirements for all parameters are fulfilled. The further away from the minimum requirements the higher values are given (up to 7) for possible tree growth (darker shading). The ECHAM5 T106 simulation produces larger areas of possible tree growth than the other simulations for Western Europe while the CLIMAP run suggests more tree growth in Eastern Europe, especially north of the Crimea area.

Unfortunately no sites with observations have been found in the areas with larger differences, France and Ukraine. The detailed contributions from the limiting factors have already been discussed above and only for Spain and Greece was a clear advantage for the T106 simulation shown. The visual impression from Fig. 10a also suggests an advantage for the ECHAM5 simulations at Duttendorf in Austria and Safarka in Slovakia, though the detailed numbers do not confirm it for the grid points next to the sites.

In Fig. 10b one can find two interesting shifts for the warm-loving trees at the eastern coast of the Black Sea and the south-western coast of the Caspian Sea with the different simulations. The likeliness of warm-loving summer-green trees shifts from the Black to the Caspian Sea from the CLIMAP to the T106 simulation which is due to a shift in the minimum temperature.

Tables 2 to 5 provide the detailed values for each site and have already been used in the discussions above. The values in the neighbourhood of the sites in these tables are the maximum values within ±1 or 3 grid points calculated for each variable separately. This leads for example in Table 3 for the ECHAM5 coupled simulation at site 6 to the discrepancy that ±1 grid point all single variables suggest possible warm-loving tree growth but not the combined score as the grid point with sufficient precipitation is different to the grid point with warm enough temperatures. For the marine sites in Table 5 only values for ±3 grid points are given, as these sites were also mostly submerged during LGM, and pollen must have been transported from further away.

In Table 6 the statistics of how many continental sites with observed tree growth agree with the likeliness of tree growth using simulation data are compared for validation purposes. Better scores are clearly obtained for the ECHAM5 T106 run for the cold-tolerant trees when looking at the grid point nearest to the site. For warm-loving trees such an advantage can only be seen for the score at ±1 grid. When extending the search to ±1.5 degrees almost all sites are verified with all simulations except the ones at Lesbos and Syria, in both cases failing on the required summer precipitation. For warm-loving trees only one failure for T106 was found, in Syria, because of summer precipitation. The statistic for warm-loving trees suffers, however, from the uncertainties in the pollen findings at three sites, as discussed above. All simulations failed to simulate possible tree growth for Urmia in Iran. We assume that the pollen found there has been blown from the coastal area of the Caspian Sea with the prevailing easterly winds in spring and early summer.

It is not clear what is the exact minimum required summer precipitation for tree growth. Laurent et al. (2004) give a range of tolerance from which one could use also a lower value than the 50 or 60 mm season^{-1} applied here. For cold-tolerant trees at the nearest grid point for T106 from the nine failures, six are due to precipitation. For the warm-loving trees a slight disadvantage exists for the coupled run.

Some genetic studies have postulated formerly unknown refugial areas by pointing to locations with a high genetic diversity, for example Crimea (Comes and Kadereit, 1998). Cordova (2007) and Cordova and Lehmann (2006) suggested that the Crimean coast was a refugium for *Alnus, Carpinus, Corylus, Quercus* and *Ulmus*, i.e. cold-tolerant summer-green trees. Their pollen data did not go as far back as the LGM but, as their earliest data at 12 000 radiocarbon years BP showed pollen from these trees, it is likely that these trees survived the LGM locally. Tsereteli et al. (1982) found pollen of warm-loving and cold-tolerant summer-green trees for the LGM in sufficient numbers to suggest that they were growing locally in Apiancha, Georgia (P. Tarasov, personal communication, 2007). Also their data record did not cover the LGM and therefore both sites are not included in our list of reliable sites; however, both sites are suggested by the model simulations as possible refugia for cold-tolerant trees. Apiancha becomes just too cold for warm-loving trees in the T106 simulation, which is not contradictory to the finding of such trees there as these findings stem from a period before the LGM.

At some sites the simulations suggest the existence of warm-loving trees while the observations report only cold-tolerant trees. Partly this is due to the fact that some *Quercus* species are warm-loving while others are cold-tolerant and if in doubt we put the observation in the cold-tolerant category. Furthermore pollen analysis has the deficiency that if one does not find pollen, it does not mean that there were no trees, especially during the LGM since the low CO_2 caused a lower pollen production (Willis et al., 2000; Leroy, 2007). However, the opposite is valid, though not always valid for the site itself due to possible long-distance transport of the pollen.

Iberia turned out to be an important area for tree refugia because of its higher summer precipitation especially in the T106 simulation compared to the present and still with warm enough winter temperatures. Quite a few sites with findings of tree pollen or charcoal confirm this model result. This has already been suggested by González-Sampériz et al. (2010) on the basis of observations.

For down-scaling we have used a method in which the difference between LGM and present-day simulations are added to a present-day climatology. Another method applicable mainly for precipitation is to multiply the ratio of LGM over present-day simulation values with a present-day climatology. This method has the advantage that it will not give any negative values for precipitation. If the simulation of the present-day is perfect, the two methods should give the same result. For the T106 simulations this method gives only slight changes with slightly higher precipitation over Iberia and slightly lower precipitation for parts of Eastern Europe. For Iberia it means that all sites in Iberia, including Gibraltar, would have received enough summer precipitation to allow the growth of trees while the values for the other sites hardly differ. The other two simulations are much more affected; they lose possible tree growth for Italy, Greece and the Caucasus area. The CLIMAP run is the most affected with a loss of most areas with possible tree growth. For consistency (using the same method for precipitation and 2m temperature) and being comparable with LA2007, we did not use this method.

5 Conclusions

In this study simulations for the present and the LGM with three ECHAM model versions are being compared. They are an ECHAM3 T42 model forced with SSTs provided by CLIMAP (1981), a coupled ECHAM5-MPIOM T31 model and a ECHAM5 T106 model forced with SSTs (corrected for systematic errors) provided by the coupled model.

The ECHAM5 T106 simulation for the present has been found in many respects superior to the other model versions, as might have been expected due to the higher resolution and the most recent model formulations but also due to corrected SSTs. The simulation of the 500 hPa height field in winter for the present gives a much better pattern in the T106 than the T31 simulation while the CLIMAP run is somewhere between the other two simulations, suggesting that in this respect the resolution is more important than other parts of the model formulations. Also the position of the subtropical jet during winter over Western Europe is much better simulated in the T106 run than in the T31 run, the latter not separating the polar from the subtropical jet.

Generally the models simulated too little precipitation for summer and winter, least serious in the T106 run. For summer the precipitation underestimation in the T106 run is, however, so weak that the model results can hardly be distinguished from estimates of the truth using observations (GPCP).

For the LGM a main difference to the CLIMAP simulations is the less cold North Atlantic and colder SSTs elsewhere in the new simulations. Reconstruction SSTs by CLIMAP (1981) and GLAMAP (Sarnthein et al., 2003) show warmer values in places of the tropics and subtropics during LGM compared with the present, which does not agree with more recent reconstructions. The coupled run shows a cooling everywhere, strongest in the Arctic areas but by far less than in CLIMAP and also less than by GLAMAP, and similar to the PMIP2 investigation (Braconnot et al., 2007). The impact was however less strong over Europe. In winter the two ECHAM5 simulations provide for the LGM over Western Europe warmer 2 m temperatures and cooler ones for Eastern Europe than simulations with the CLIMAP SSTs.

For T106 during winter the Alaskan ridge and the trough over eastern US were both much stronger during the LGM than NOW. The coupled model shows similar patterns while the simulation with CLIMAP SSTs is very different: the ridge over Western Europe, shown for the present, is completely wiped out for the LGM. For summer the changes from NOW to LGM are less pronounced. A slight ridging over Eastern Europe during LGM might be of importance. The polar jet over Western Europe (30° W–10° E) moves in the T106 simulation from about 50° N for the present to 40° N during LGM which is probably realistic. In the CLIMAP run it is considerably strengthened at the LGM at the same latitude as for the present-day. Common to all simulations is an increase of wind speed in the Trade Winds in summer and an increase in the North Atlantic westerlies in winter for the LGM.

Large-scale differences have been noted in the simulated minimum temperature between the different runs. It was not possible to state if this is more realistic in the one or the other simulation because of lack of observation data. The precipitation for Europe during LGM in winter is characterized by a change in the direction of the main passage of cyclones. In the CLIMAP run, cyclones move from the British Isles straight to the east into central Europe instead of towards the north-east as for the present. In the ECHAM5 T106 run, the main cyclone passage is towards the eastern Mediterranean Sea which is probably a realistic feature as the eastern Mediterranean was more humid during LGM than now, evident from a high stand of the Dead Sea and other lakes during LGM. For summer the simulations suggest mostly less precipitation during LGM than for the present. The ECHAM5 T106 run clearly has the highest amount of precipitation, and more precipitation during LGM than NOW for Western Europe.

The main emphasis of the study is on the comparison between possible summer-green tree growth from pollen and charcoal analyses and model estimates using summer precipitation, minimum winter temperatures and growing degree days (above 5 °C). More sites with palaeo-observations of tree growth during the LGM agree with areas of possible tree growth suggested by the ECHAM5 T106 simulations than by the other simulations. This is especially true for Iberia but less conclusive for the rest of Europe. The clear message especially from the ECHAM5 T106 simulations is that warm-loving summer-green trees could have survived mainly in Spain but also in Greece in agreement with findings of pollen or charcoal during LGM. Southern Italy is also suggested by the models as possible refugium for warm-loving summer-green trees, but no reliable sites with observational evidence were available to prove it.

Having gained confidence in the usage of the climate model simulations for identifying possible refugia, it might be useful to extend the investigation to other areas of the world.

Acknowledgements. We are grateful to many individuals and institutions who provided data and information useful to our study. The Deutsche Forschungsgemeinschaft funded part of this work in the project MISO within the DFG Priority Programme 1266 (INTERDYNAMIK). The simulations were performed at the "Deutsches Klimarechenzentrum" in Hamburg, Germany. The computing time for the T106 simulations was financed by the German ministry of education and research under contract number 438-BMBF.

The service charges for this open access publication
have been covered by the Max Planck Society.

References

Arpe, K., Hagemann, S., and Jacob, D.: The realism of the ECHAM5 models to simulate the hydrological cycle in the Arctic and North European area, Nordic Hydrology, 36, 349–367, 2005.

Aura Tortosa, J. E., Jordá Pardo, J. F., Pérez Ripoll, M., Rodrigo García, M. J., Badal García, E., and Guillem Calatayud, P.: The far south: the Pleistocene-Holocene transition in Nerja Cave (Andalucía, Spain), Quat. International, 93–94, 19–30, 2002.

Beaudouin, C., Jouet, G., Suc, J.-P., Berné, S., and Escarguel, G.: Vegetation dynamics in southern France during the last 30 ky BP in the light of marine palynology, Quat. Sci. Rev., 26(7–8), 1037–1054, 2007.

Boessenkool, K. P., Brinkhuis, H., Schonfeld, J., and Targarona, J.: North Atlantic sea-surface temperature changes and the climate of western Iberia during the last deglaciation; a marine palynological approach, Global Planet. Change, 30(1), 33–39, 2001.

Bottema, S.: Pollen analytical investigations in Thessaly (Greece), Palaeohistoria, 21, 19–40, 1979.

Buccheri, G., Capretto, G., Di Donato, V., Esposito, P., Ferruzza, G., Pescatore, T., Russo Ermolli, E., Senatore, M. R., Sprovieri, M., Bertoldo, M., Carella, D., and Madonia, G.: A high resolution record of the last deglaciation in the southern Tyrrhenian Sea: environmental and climatic evolution, Mar. Geology, 186, 447–470, 2002.

Braconnot, P., Otto-Bliesner, B., Harrison, S., Joussaume, S., Peterchmitt, J.-Y., Abe-Ouchi, A., Crucifix, M., Driesschaert, E., Fichefet, Th., Hewitt, C. D., Kageyama, M., Kitoh, A., Lané, A., Loutre, M.-F., Marti, O., Merkel, U., Ramstein, G., Valdes, P., Weber, S. L., Yu, Y., and Zhao, Y.: Results of PMIP2 coupled simulations of the Mid-Holocene and Last Glacial Maximum – Part 1: experiments and large-scale features, Clim. Past, 3, 261–277, 2007, http://www.clim-past.net/3/261/2007/.

Canali, G., Capraro, L., Donnici, S., Rizzetto, F., Serandrei-Barbero, R., and Tosi, L.: Vegetational and environmental changes in the eastern Venetian coastal plain (Northern Italy) over the past 80 000 years. Palaeogeography, Palaeoclimatology, Palaeoecology, 253(3–4), 300–316, 2007.

Carrión, J. S.: Patterns and process of late Quaternary environmental change in a montane region of south Western Europe, Quat. Sci. Rev., 21, 2047–2066, 2002.

Carrión, J. S., Finlayson, C., Fernández, S., Finlayson, G., Allué, E., López-Sáez, J. A., López-García, P., Gil-Romera, G., Bailey, G., and González-Sampériz, P.: A coastal reservoir of biodiversity for Upper Pleistocene human populations: palaeoecological investigations in Gorham's Cave (Gibraltar) in the context of the Iberian Peninsula, Quat. Sci. Rev., 27, 2118–2135, 2008.

CERA: http://cera-www.dkrz.de/CERA/index.html, last accessed 7 February 2010.

CLIMAP: Seasonal reconstructions of the Earth's surface at the last glacial maximum, Geological Society of America, Map Chart Ser, MC-36, 1981.

Combourieu-Nebout, N., Paterne, M., Turon, J.-L., and Siani, G.: A high-resolution record of the last deglaciation in the central Mediterranean Sea: Palaeovegetation and palaeohydrological evolution, Quat. Sci. Rev., 17(4), 303–317, 1998.

Comes, H. P. and Kadereit, J. W.: The effect of Quaternary climatic changes on plant distribution and evolution, Trends in Plant Sciences, 3, 432–438, 1998.

Cordova, C. E.: Holocene mediterranization of the southern Crimean vegetation: Paleoecological records, regional climate change, and possible non-climatic influences. The Black Sea Flood Question: Changes in Coastline, climate and Human Settlement, edited by: Yanko-Hombach, V., Gilbert, A., Panin, N., and Dolukhanov, P., NATO Science Series IV – Earth and Environmental Sciences, Springer, 319–344, 2007.

Cortés-Sánchez, M., Morales-Muñiz, A., Simón-Vallejo, M. D., Bergadà-Zapata, M., Delgado-

Huertas, A., López-García, P., López-Sáez, J. A., Lozano-Francisco, M. C., Riquelme-Cantal, J. A., Roselló-Izquierdo, E., Sánchez-Marco, A., and Vera-Peláez, J. L.: Palaeoenvironmental and cultural dynamics of the coast of Málaga (Andalusia, Spain) during the Upper Pleistocene and early Holocene, Quat. Sci. Rev., 27(23–24), 2176–2193, 2008.

Djamali, M., de Beaulieu, J.-L., Shah-Hosseini, M., Andrieu-Ponel, V., Ponel, P., Amini, A., Akhani, H., Leroy, S. A. G, Stevens, L., Lahijani, H., and Brewer S.: A Late Pleistocene long pollen record from Lake Urmia, NW Iran, Quat. Res., 69, 413–420, 2008.

Filipova-Marinova, M.: Paleoenvironmental changes along the southern Black Sea coast of Bulgaria during the last 29000 years, Phytologia Balcanica, 9(2), 275–292, 2003.

Fletcher, W. J. and Sánchez-Goñi, M. F.: Orbital- and sub-orbital-scale climate impacts on vegetation of the western Mediterranean basin over the last 48,000 yr, Quat. Res., 70, 451–464, 2008.

Florineth, D. and Schlüchter, C.: Alpine Evidence for Atmospheric Circulation Patterns in Europe during the Last Glacial Maximum, Quat. Res., 54, 295–308, 2000.

Gates, W. L.: AMIP: The Atmospheric Model Intercomparison Project, B. Am. Meteorol. Soc., 73, 1962–1970, 1992.

Geraga, M., Ioakim, Chr., Lykousis, V., Tsaila-Monopolis, St., and Mylona, G.: The high-resolution palaeoclimatic and palaeoceanographic history of the last 24,000 years in the central Aegean Sea, Greece, Palaeogeography, Palaeoclimatology, Palaeoecology, 287, 101–115, 2010.

González-Sampériz, P., Leroy, S. A. G., Fernández, S., García-Antón, M., Gil-García, M. J., and Uzquiano, P.: Valero-Garcés B., Figueiral I.: Steppes, savannahs, forests and phytodiversity reservoirs during the Pleistocene in the Iberian Peninsula, Rev. Palyn. Palaeobot, in press, 2010.

González-Sampériz, P., Valero-Garcés, B., Carrión, J., Peña-Monné, J. L., García-Ruiz, J. M., and Martí-Bono, C.: Glacial and Lateglacial vegetation in Northeastern Spain: new data and a review, Quat. International, 140–141, 4–20, 2005.

Grosswald, M. G.: Late Weichselian ice sheet of northern Eurasia, Quat. Res., 13, 1–32, 1980.

Hammer, C. U., Andersen, K. K., Clausen, H. B., Dahl-Jensen, D., Hvidberg, C. S., and Iversen, P.: The stratigraphic dating of the GRIP ice core. Special Report of the Geophysical Department, Niels Bohr Institute for Astronomy, Physics and Geophysics, University of Copenhagen, GRIP-GISP CD-ROM (file gripstrt), 1997.

Huffman, G. J., Adler, R. F., Arkin, P. A., Chang, A., Ferraro, R., Gruber, A., Janowiak, J., Joyce, R.J., McNab, A., Rudolf, B., Schneider, U., and Xie, P.: The Global Precipitation Climatology Project (GPCP) combined precipitation data set, B. Am. Meteorol. Soc., 78, 5–20, 1996.

Jankovská, V. and Pokorný, P.: Forest vegetation of the last full-glacial period in the Western Carpathians (Slovakia and Czech Republic), Preslia, 80, 307–324, 2008.

Kaltenrieder, P., Belis, C. A., Hofstetter, S., Ammann, B., Ravazzi, C., and Tinner, W.: Environmental and climatic conditions at a potential Glacial refugial site of tree species near the Southern Alpine glaciers. New insights from multiproxy sedimentary studies at Lago della Costa (Euganean Hills, Northeastern Italy), Quat. Sci. Rev., 28, 2647–2662, 2009.

Kelts, K. and Shahrabi, M.: Holocene sedimentalogy of hypersaline Lake Urmia, northwestern Iran, Paleogeography, Paleoclimatology and Paleoecology, 54, 105–130, 1986.

Kotthoff, U., Müller, U. C., Pross, J., Schmiedl, G., Lawson, I. T., van de Schootbrugge, B., and Schulz, H.: Lateglacial and Holocene vegetation dynamics in the Aegean region: an integrated view based on pollen data from marine and terrestrial archives, The Holocene, 18, 1019–1032, 2008.

Kucera, M., Weinelt, M., Kiefer, T., Pflaumann, U., Hayes, A., Chen, M. T., Mix, A. C., Barrows, T. T., Cortijo, E., Duprat, J., Juggins, S., and Waelbroeck, C.: Reconstruction of Sea-Surface Temperatures from Assemblages of Planktonic Foraminifera: Multi-Technique Approach Based on Geographically Constrained Calibration Data Sets and Its Application to Glacial Atlantic and Pacific Oceans, Quat. Sci. Rev., 24, 951–998, 2005.

Leemans, R. and Cramer, W.: The IIASA database for mean monthly values of temperature, precipitation and cloudiness of a global terrestrial grid, International Institute for Applied Systems Analysis (IIASA), RR-91-18, 1991.

Leroy, S. A. G.: Progress in palynology of the Gelasian-Calabrian Stages in Europe: ten messages, Revue de Micropaléontologie, 50, 293–308, 2007.

Leroy, S. A. G. and Arpe, K.: Glacial refugia for summer-green trees in Europe and S-W Asia as proposed by ECHAM3 time slice atmospheric model simulations, J. Biogeography, 34, 2115–2128. doi:10.1111/j.1365-2699.2007.01754x, 2007.

Lorenz, S., Grieger, B., Helbig, P., and Herterich, K.: Investigating the sensitivity of the Atmospheric Global circulation Model ECHAM3 to paleoclimatic boundary conditions, Geologische Rundschau, 85, 513–524, 1996.

Lucchi, M. R.: Vegetation dynamics during the Last Interglacial-Glacial cycle in the Arno coastal plain (Tuscany, western Italy): location of a new tree refuge, Quat. Sci. Rev., 27, 2456–2466, 2008.

Margari, V., Gibbard, P. L., Bryant, C. L., and Tzedakis, P. C.: Character of vegetational and environmental changes in southern Europe during the last glacial period; evidence from Lesvos Island, Greece, Quat. Sci. Rev., 28, 1317–1339, 2009.

Mikolajewicz, U., Vizcaino, M., Jungclaus, J., and Schurgers, G.: Effect of ice sheet interactions in anthropogenic climate change simulations, Geophys. Res. Lett., 34, L18706, doi:10.1029/2007GL031173, 2007.

Miola, A., Bondesan, A., Corain, L., Favaretto, S., Mozzi, P., Piovan, S., and Sostizzo, I.: Wetlands in the Venetian Po Plain (northeastern Italy) during the Last Glacial Maximum: Interplay between vegetation, hydrology and sedimentary environment, Rev. Palaeobotany and Palynology, 141, 53–81, 2006.

Mix, A. C., Bard, E., and Schneider, R.: Environmental processes of the ice age: land, oceans, glaciers (EPILOG), Quat. Sci. Rev., 20, 627–657, 2001.

Niklewski, J. and Van Zeist, W.: A Late Quaternary pollen diagram from northwestern Syria, Acta Bot. Neerl., 19(5), 737–754, 1970.

Okuda, M., Yasuda, Y., and Setoguchi, T.: Middle to Late Pleistocene vegetation history and climatic changes at Lake Kopais, Southeast Greece, Boreas, 30(1), 73–82, 2001.

Otto-Bliesner, B. L., Schneider, R., Brady, E. C., Kucera, M., Abe-Ouchi, A., Bard, E., Braconnot, P., Crucifix, M., Hewitt, C.D., Kageyama, M., Marti, O., Paul, A., Rosell-Melé, A., Waelbroeck, C., Weber, S. L., Weinelt, M., and Yu, Y.: A comparison of PMIP2 model simulations and the MARGO proxy reconstruction for tropical sea surface temperatures at last glacial maximum, Clim. Dynam., 32, 799–815, 2009.

Pantaleón-Cano, J., Yll, E.I., Pérez-Obiol, R., and Roure, J. M.: Palynological evidence for vegetational history in semi-arid areas of the western Mediterranean (Almeria, Spain), The Holocene, 13, 109–119, 2003.

Paganelli, A.: Evolution of vegetation and climate in the Veneto-Po plain during the late-glacial and the Early Holocene using pollen-stratigraphic data, Il Quaternario, 9(2), 581–590, 1996.

Peltier, W. R.: Global glacial isostasy and the surface of the ice-age Earth: the ICE-5G (VM2) model and GRACE, Annu. Rev. Earth Planet. Sci., 32, 111–149, 2004.

Pons, A. and Reille, M.: The Holocene and Upper Pleistocene pollen record from Padul (Granada, Spain): a new study, Palaeogeography, Palaeoclimatology, Palaeoecology, 66, 243–263, 1988.

Peyron, O., Guiot, J., Cheddadi, R., Tarasov, P., Reille, M., de Beaulieu, J.-L., Bottema, S., and Andrieu, V.: Climatic Reconstruction in Europe for 18,000 YR B.P. from Pollen Data, Quat.

Res., 49, 183–196, 1998.

Roeckner, E., Bäuml, G., Bonaventura, L., Brokopf, R., Esch, M., Giorgetta, M., Hagemann, S., Kirchner, I., Kornblueh, L., Manzini, E., Rhodin, A., Schlese, U., Schulzweida, U., and Tompkins, A.: The atmospheric general circulation model ECHAM5, Part I: Model description, Max Planck Institute for Meteorology, Hamburg, Report no. 349, 2003.

Roeckner, E., Stier, P., Feichter, J., Kloster, S., Esch, M., and Fischer-Bruns, I.: Impact of Carbonaceous aerosol forcing on regional climate change, J. Clim. Dynam., 27, 553–571, doi:10.1007/s00382-006-0147-3, 2006.

Rossignol-Strick, M. and Planchais, N.: Climate patterns revealed by pollen and oxygen isotope records of a Tyrrhenian sea core, Nature, 342, 413–416, 1989.

Roucoux, K. H., de Abreu, L., Shackleton, N. J., and Tzedakis, P. C.: The response of NW Iberian vegetation to North Atlantic climate oscillations during the last 65 kyr, Quat. Sci. Rev., 24, 1637–1653, 2005.

Ruiz Zapata, M. B., Gil García, M. J., Dorado Valiño, M., Valdeolmillos Rodríguez, A., and Pérez-González, A.: Clima y vegetación durante el Pleistoceno superior y el Holoceno en la Sierra de Neila (Sistema Ibérico Noroccidental), Cuaternario y Geomorfología, 16(1–4), 9–20, 2002.

Sarnthein, M., Gersonde, R., Niebler, S., Pflaumann, U., Spielhagen, R., Thiede, J., Wefer, G., and Weinelt, M.: Overview of Glacial Atlantic Ocean Mapping (GLAMAP 2000), Paleoceanography, 18(2), 1030, 8/1-6, doi:10.1029/2002PA000769, 2003.

Starnberger, R., Terhorst, B., Rähle,W., Peticzka, R., and Haas, J. N.: Palaeoecology of Quaternary periglacial environments during OIS-2 in the forefields of the Salzach Glacier (Upper Austria), Quat. International, 198, 51–61, 2009.

Stein, M., Torfstein, A., Gavrieli, I., and Yechieli, Y.: Abrupt aridities and salt deposition in the post-glacial Dead Sea and their North Atlantic connection, Quat. Sci. Rev., 1–9, doi:10.1016/j.quascirev.2009.10.015, 2009.

Targarona, J.: Climatic and Oceanographic Evolution of the Mediterranean Region Over the Last Glacial-Interglacial Transition. A Palynological Approach, LPP Contribution Series, No. 7, Utrecht, 1997.

Tinner, W., Hubschmid, P., Wehrli, M., Ammann, B., and Conedra, M.: Long-term forest fire ecology and dynamics in southern Switzerland, J. Ecol., 87, 273–289, 1999.

Turon, J.-L., Lézine, A.-M., and Denèfle, M.: Land-sea correlations for the last glaciation inferred from a pollen and dinocyst record from the Portuguese margin, Quat. Res., 59, 88–96, 2003.

Tsereteli, L. D., Klopotovskaya, N. B., and Kurenkova, E. L.: Mnogosloinaya arheologicheskaya stoyanka Apiancha (Abkhazia), in: Chetvertichnaya sistema Gruzii, Metsniereba, Tbilisi, 198–212, 1982 (in Russian).

Tzedakis, P. C.: Vegetation change through glacial-interglacial cycles; a long pollen sequence perspective, Philosophical Transactions of the Royal Society, London, B, 345, 403–432, 1994.

Tzedakis, P. C.: The last climatic cycle at Kopais, central Greece, J. Geol. Soc., London, 155, 425–434, 1999.

Uppala, S. M., Kållberg, P. W., Simmons, A. J., Andrae, U., da Costa Bechtold, V., Fiorino, M., Gibson, J. K., Haseler, J., Hernandez, A., Kelly, G. A., Li, X., Onogi, K., Saarinen, S., Sokka, N., Allan, R. P., Andersson, E., Arpe, K., Balmaseda, M. A., Beljaars, A. C. M., van de Berg, L., Bidlot, J., Bormann, N., Caires, S., Chevallier, F., Dethof, A., Dragosavac, M., Fisher, M., Fuentes, M., Hagemann, S., Hólm, E., Hoskins, B. J., Isaksen, L., Janssen, P. A. E. M., Jenne, R., McNally, A. P., Mahfouf, J.-F., Morcrette, J.-J., Rayner, N. A., Saunders, R. W., Simon, P., Sterl, A., Trenberth, K. E., Untch, A., Vasiljevic, D., Viterbo, P., and Woollen, J.: The ERA-40 re-analysis, Q. J. Roy. Meteorol. Soc., 131, 2961–3012, doi:10.1256/qj.04.176, 2005.

Uzquiano, P.: L'Homme et le bois au Paléolithique en région Cantabrique, Espagne. Exemples d'Altamira et d'El Buxu, Bulletin de la Société Botanique de France, 139, 361–372, 1992.

Van Campo, M.: Relations entre la Végétation de l'Europe et les températures de surface océaniques après le dernier maximum glaciaire, Pollen et Spores, XXVI(3–4), 497–518, 1984.

Wagner, B., Lotter, A. F., Nowaczyk, N., Reed, J. M., Schwalb, A., Sulpizio, R., Valsecchi, V., Wessels, M., and Zanchetta, G.: A 40,000-year record of environmental change from ancient Lake Ohrid (Albania and Macedonia), J. Paleolimnol., 41, 407–430, 2009.

Watts, W. A., Allen, J. R. M., Huntley, B., and Fritz, S. C.: Vegetation history and climate of the last 15,000 years at Lagho di Monticchio, southern Italy, Quat. Sci. Rev., 15, 113–132, 1996.

Willis, K. J., Rudner, E., and Sümeg, P.: The Full-Glacial Forests of Central and Southeastern Europe, Quat. Res., 53, 203–213, 2000.

Yokoyama, Y., Lambeck, K., de Dekhar, P., Johnston, P., and Fifield, L. K.: Timing of last glacial maximum from observed sea level minima, Nature, 406, 713–716, 2000.

Table 1. Reliable continental and marine sites with summer-green tree growth during LGM from west to east. In column 'tree' the letters W mean warm-loving trees and C cold-tolerant trees. The evidence of tree growth comes mostly from pollen analysis, except sites 3 (Altamira) and 4 (Nerja) which have findings of charcoal, and site 1 (Gibraltar) which has evidence from pollen and fossil wood.

No	long	lat	site	seas/city/country	water depth/altitude	tree	author
Group I: reliable continental sites							
1	−5.30	36.02	Gorham's cave	Gibraltar	0	W+C	Carrión et al. (2008)
2	−4.70	36.80	Bajondillo	S. Spain	0–80	W+C	Cortés Sánchez et al. (2008)
3	−4.11	43.38	Altamira	N. Spain	70	C	Uzquiano (1992)
4	−3.81	36.75	Nerja	S. Spain	158	W	Aura Tortosa et al. (2002)
5	−3.67	37.00	Padul	S. Spain	785	C	Pons and Reille (1988)
6	−2.66	36.77	San Rafael	S. Spain	0	W+C	Pantaleón-Cano et al. (2003)
7	−2.30	38.24	Siles	S. Spain	1320	C someW	Carrión (2002)
8	−0.40	42.73	Tramacastilla	NE Spain	1640	C	González-Sampériz et al. (2005)
9	−0.40	42.99	Formigal	NE Spain	1585	C	IBID
10	3.18	42.04	Laguna Grande	N. Spain	1510	W+C	Ruiz Zapata et al. (2002)
11	8.81	46.00	L. di Origlio	Switzerland	416	C	Tinner et al. (1999)
12	11.43	45.29	Po valle	Italy	19	C	Paganelli (1996)
13	11.75	45.27	Lago della Costa	Italy, Po	7	C	Kaltenrieder et al. (2009)
14	12.83	48.16	Duttendorf	Austria	420	C	Starnberger et al. (2009)
15	15.60	40.94	L. Monticchio	Neaple Italy	1326	C	Watts et al. 1996
16	20.57	48.85	Safarka	NE Slovakia	600	C	Jankovska and Pokorny (2008)
17	20.80	40.90	L. Ohrid	Albania	693	C	Wagner et al. (2009)
18	20.91	39.65	Ioannina	Greece	470	C some W	Tzedakis (1994)
19	22.27	39.50	Xinias	Greece	480	C some W	Bottema (1979)
20	23.05	39.44	Kopais	Greece	95	C	Tzedakis (1999), Okuda et al. (2001)
21	26.30	39.10	Lesvos ML01	Lesbos Greece	323	C	Margari et al. (2009)
22	36.30	35.07	Ghab	NW Syria	240	W+C	Niklewski and Van Zeist (1970)
23	45.33	37.75	Urmia BH2&BH3	NW Iran	1310	C	Djamali et al. (2008)
Group II: reliable marine corings							
24	−10.33	40.57	MD95-2039	off Portugal	−3381	C	Roucoux et al. (2005)
25	−10.20	37.77	SU81-18	off Portugal	−3135	C	Turon et al. (2003)
26	−9.51	37.93	SO75-6KL	off SW Iberia	−1281	C	Boessenkool et al. (2001)
27	−2.62	36.14	MD95-2043	Alboran Sea	−1841	C	Fletcher and Sánchez-Goñi (2008)
28	3.72	42.82	MD99-2349	Gulf of Lions	−126	C	Beaudouin et al. (2007)
29	3.87	42.70	MD99-2348 PRGL1-4	Gulf of Lions	−296	C	Beaudouin et al. (2007)
30	14.49	38.82	KET8003	Tyrrhenian Sea	−1900	C	Rossignol-Strick and Planchais (1989)
31	14.70	40.47	C106	Tyrrhenian Sea	−292	C	Buccheri et al. (2002)
32	17.62	41.29	MD90-917	Adriatic Sea	−1010	C	Combourieu-Nebout et al. (1998)
33	17.91	41.79	IN68-9	Adriatic Sea	−1234	C	Targarona (1997)
34	24.61	40.09	SL152	N. Aegean Sea	−978	C some W	Kotthoff et al. (2008)
35	25.00	39.26	MNB3	Aegean Sea	−800	C	Geraga et al. (2010)
36	28.32	42.40	C-2345	W. Black Sea	−122	C	Filipova-Marinova (2003)

Table 2. Summary of ECHAM5 T106 run using JJA precipitation, minimum temperature and growing degree days above 5 °C (GDD5) for continental sites. Values at the nearest grid point of the sites as well as maximum values within a distance ±1 or 3 grid points are given for each variable. Unknown values are marked by ****. The sort of trees found during LGM are given by W for warm-loving trees and C for cold-tolerant trees.

	Distance from site															
	0	±1	±3	0	±1	±3	0	±1	±3	0	±1	±3	0	±1	±3	
no	precip			T_{min}			GDD5			cool score			warm score			obs
1	36	48	139	6.7	7.4	9.3	2471	2612	3153	0	0	6	0	0	6	WC
2	98	139	139	5.3	7.4	7.4	2202	2612	3526	2	6	6	4	4	6	WC
3	123	172	233	1.3	1.5	2.6	1705	1705	2531	6	6	6	4	4	6	C
4	52	98	175	5.1	5.3	7.4	2290	2289	3526	1	2	6	0	4	6	WC
5	46	132	175	4.3	5.1	7.4	2190	2289	3526	0	4	6	0	2	4	C
6	32	148	175	4.9	6.7	7.6	2419	2899	3526	0	4	6	0	2	4	WC
7	175	175	175	−0.4	2.4	6.7	1031	1678	2899	5	4	6	2	2	4	WC
8	168	364	437	−1.8	3.2	3.8	932	1971	2551	5	4	6	0	4	6	C
9	273	369	437	−3.7	3.2	3.8	509	1971	2551	0	6	6	0	4	6	C
10	144	204	344	4.6	4.6	4.6	2896	2896	2896	6	6	6	6	6	6	WC
11	322	562	580	−7.6	−7.0	−2.4	1404	1591	1621	6	6	6	0	0	2	C
12	188	342	574	−8.9	−6.6	−2.9	1547	1754	1754	7	6	6	0	0	0	C
13	183	334	574	−9.0	−7.9	−2.9	1603	1754	1754	7	6	6	0	0	0	C
14	699	698	698	−15.1	−12.7	−12.0	299	720	943	0	0	4	0	0	0	C
15	121	131	181	−4.0	−0.5	2.9	1140	2024	2591	5	6	6	0	4	6	C
16	393	509	509	−18.2	−15.3	−14.0	657	1246	1536	0	0	6	0	0	0	C
17	120	147	226	−7.0	−4.8	2.1	973	1184	2512	4	4	6	0	0	4	C
18	57	114	131	2.1	2.1	3.6	2432	2432	2924	1	4	5	0	4	4	WC
19	60	88	131	0.1	0.1	3.8	2513	2512	2979	1	2	5	0	4	4	WC
20	63	75	131	−0.3	0.2	3.8	2352	2512	2979	1	2	5	2	2	4	C
21	***	18	47	*****	3.2	3.2	****	2946	2946	*	0	0	*	0	0	C
22	5	10	32	5.6	7.6	8.9	3106	3522	3942	0	0	0	0	0	0	WC
23	20	28	83	−6.4	−5.2	2.6	2005	2310	3950	0	0	2	0	0	0	C

Table 3. Same as Table 2 for ECHAM5 T31 coupled.

	Distance from site																
	0	±1	±3	0	±1	±3	0	±1	±3	0	±1	±3	0	±1	±3	
no	precip			T_{min}			GDD5			cool score			warm score			obs
1	32	45	136	5.1	5.9	7.2	1545	1649	2349	0	0	5	0	0	2	WC
2	94	136	136	3.3	5.9	6.8	1285	1649	2276	2	4	5	2	2	2	WC
3	70	117	153	−0.3	−0.1	1.1	967	967	1852	1	3	6	0	0	4	C
4	46	93	167	3.3	3.3	6.8	1303	1302	2276	0	2	5	0	2	2	WC
5	40	125	167	2.5	3.3	6.8	1235	1302	2276	0	1	4	0	0	2	C
6	26	142	167	3.2	5.2	6.8	1404	1826	2276	0	1	3	0	0	2	WC
7	168	167	167	−2.3	0.4	5.2	559	970	1826	0	2	3	0	0	2	WC
8	111	281	355	−2.8	2.1	2.7	541	1389	1721	0	1	6	0	2	4	C
9	190	281	355	−4.6	2.1	2.7	176	1340	1721	0	2	6	0	0	4	C
10	128	178	293	4.8	4.8	5.3	2392	2391	2391	6	6	6	6	6	6	WC
11	244	477	488	−7.0	−6.5	−2.0	1046	1230	1241	5	5	6	0	0	0	C
12	130	274	497	−6.3	−4.7	0.0	1190	1412	1412	5	5	5	0	0	2	C
13	129	270	497	−5.8	−4.8	0.0	1250	1412	1412	5	5	6	0	0	2	C
14	625	625	625	−13.9	−11.8	−10.0	76	389	572	0	0	0	0	0	0	C
15	98	110	152	−4.5	−1.0	1.9	706	1552	1950	0	3	3	0	2	2	C
16	276	402	402	−15.4	−12.4	−10.5	492	1058	1421	0	4	4	0	0	0	C
17	105	121	195	−8.9	−7.1	−0.1	769	988	2140	0	3	6	0	0	0	C
18	47	109	123	−0.1	−0.1	2.9	1912	1912	2341	0	3	4	0	0	0	WC
19	59	87	123	−1.8	−1.8	2.9	2141	2140	2419	1	2	4	0	0	2	WC
20	64	75	123	−2.7	−1.8	2.9	2005	2140	2419	1	2	4	0	2	2	C
21	***	19	47	*****	0.4	0.9	****	2593	2593	*	0	0	*	0	0	C
22	4	10	31	3.3	4.8	6.1	2406	2762	3156	0	0	0	0	0	0	WC
23	22	30	95	−6.3	−5.4	1.4	1592	1832	3229	0	0	2	0	0	0	C

Title Page
Abstract
Introduction
Conclusions
References
Tables
Figures
◀◀
▶▶
◀
▶
Back
Close
Full Screen / Esc
Printer-friendly Version
Interactive Discussion

Table 4. Same as Table 2 for the ECHAM3 T42 CLIMAP run.

	Distance from site															
	0	±1	±3	0	±1	±3	0	±1	±3	0	±1	±3	0	±1	±3	
no	precip			T_{min}			GDD5			cool score			warm score			obs
1	17	27	124	7.1	8.2	8.9	2899	3165	3858	0	0	6	0	0	6	WC
2	73	120	124	6.1	8.2	9.9	2763	3165	3963	1	6	6	2	6	6	WC
3	−6	38	67	−3.4	−3.1	0.9	1583	1583	2699	0	0	1	0	0	2	C
4	20	72	127	6.3	6.3	9.9	2809	2809	3963	0	1	6	0	2	6	WC
5	9	90	127	5.8	6.3	9.9	2665	2809	3963	0	2	6	0	2	6	C
6	−15	100	127	6.8	8.8	9.9	2900	3309	3963	0	4	5	0	2	4	WC
7	127	127	127	1.2	3.7	8.8	1459	2115	3309	5	5	5	2	2	4	WC
8	18	181	253	−4.0	0.9	0.9	1126	2051	2367	0	0	6	0	0	4	C
9	92	181	253	−7.1	0.4	0.9	686	2051	2367	0	6	6	0	0	4	C
10	90	121	219	4.3	4.3	4.6	2553	2552	2552	2	6	6	4	6	6	WC
11	125	344	367	−7.8	−7.3	−2.3	1517	1695	1782	6	6	6	0	0	2	C
12	46	171	395	−6.6	−4.9	0.2	1758	2045	2045	0	6	6	0	0	4	C
13	48	170	395	−6.3	−5.2	0.2	1827	2045	2087	0	6	6	0	0	4	C
14	543	542	542	−15.3	−12.7	−10.6	197	461	968	0	0	4	0	0	0	C
15	78	89	129	−3.1	0.5	3.6	1303	2269	2822	2	2	4	0	4	4	C
16	275	397	397	−13.5	−10.4	−8.0	157	674	1118	0	0	3	0	0	0	C
17	52	68	122	−6.1	−4.7	2.6	1393	1539	2715	1	1	3	0	0	0	C
18	13	69	74	2.6	2.6	6.2	2569	2568	3010	0	1	1	0	0	2	WC
19	28	62	76	1.1	1.1	6.2	2715	2715	3010	0	1	2	0	2	2	WC
20	34	50	76	0.7	1.1	6.2	2545	2715	3010	0	1	2	0	0	2	C
21	***	5	25	*****	5.4	5.7	****	3006	3006	*	0	0	*	0	0	C
22	3	8	29	6.0	8.1	9.6	3226	3626	4019	0	0	0	0	0	0	WC
23	13	22	54	−4.8	−3.6	3.2	2203	2466	4051	0	0	1	0	0	0	C

Table 5. Summary of all simulations for marine sites using JJA precipitation, minimum temperature (Tmin) and growing degree days above 5 °C (GDD5). Only maximum values within a distance ±3 grid points are given for each variable.

	T106					coupled					CLIMAP					
				score					score					score		tree
Site no	prec	T_{min}	GGD5	C	W	prec	T_{min}	GGD5	C	W	prec	T_{min}	GGD5	C	W	obs
24	37	7.8	2420	0	0	30	5.7	1508	0	0	16	5.6	1895	0	0	C
25	41	8.2	2573	0	0	33	6.0	1591	0	0	18	6.7	2077	0	0	C
26	41	8.2	2573	0	0	33	6.0	1591	0	0	20	6.7	2077	0	0	C
27	148	7.8	3526	4	2	142	6.8	2276	1	0	100	9.9	3963	4	2	C
28	344	4.6	2896	6	6	293	5.3	2391	6	6	219	4.6	2552	6	6	C
29	293	4.6	2896	6	6	253	4.8	2391	6	6	187	4.3	2552	6	6	C
30	131	5.1	2901	4	4	110	3.8	2074	1	2	89	6.9	3298	2	0	C
31	181	3.1	2378	6	6	152	2.4	1694	3	2	129	4.0	2448	4	4	C
32	238	2.9	2617	6	6	185	1.3	1950	4	4	118	3.4	2822	3	2	C
33	291	2.9	2617	6	6	225	0.8	1950	6	4	151	1.9	2822	4	2	C
34	134	3.7	2964	5	4	132	0.2	2398	5	2	91	4.0	2872	2	2	WC
35	89	3.8	2979	2	4	95	1.2	2419	2	2	76	4.5	2883	2	2	C
36	160	−5.1	2108	6	0	147	−6.3	2121	6	0	84	1.8	2371	2	0	C

Table 6. Number of continental sites with observed tree growth where the simulations suggest possible tree growth at the grid point nearest to the site (0), within ±1 grid point, and within ±3 grid points (±1.5°) from the site.

Cold-tolerant trees									
obs.	ECHAM5	T106		ECHAM5	T31		ECHAM3	T42	CLIMAP
	0	±1	±3	0	±1	±3	0	±1	±3
23	14	17	21	8	18	20	6	15	21
Warm-loving trees									
obs.	ECHAM5	T106		ECHAM5	T31		ECHAM3	T42	CLIMAP
	0	±1	±3	0	±1	±3	0	±1	±3
9	3	7	8	2	3	7	3	6	8

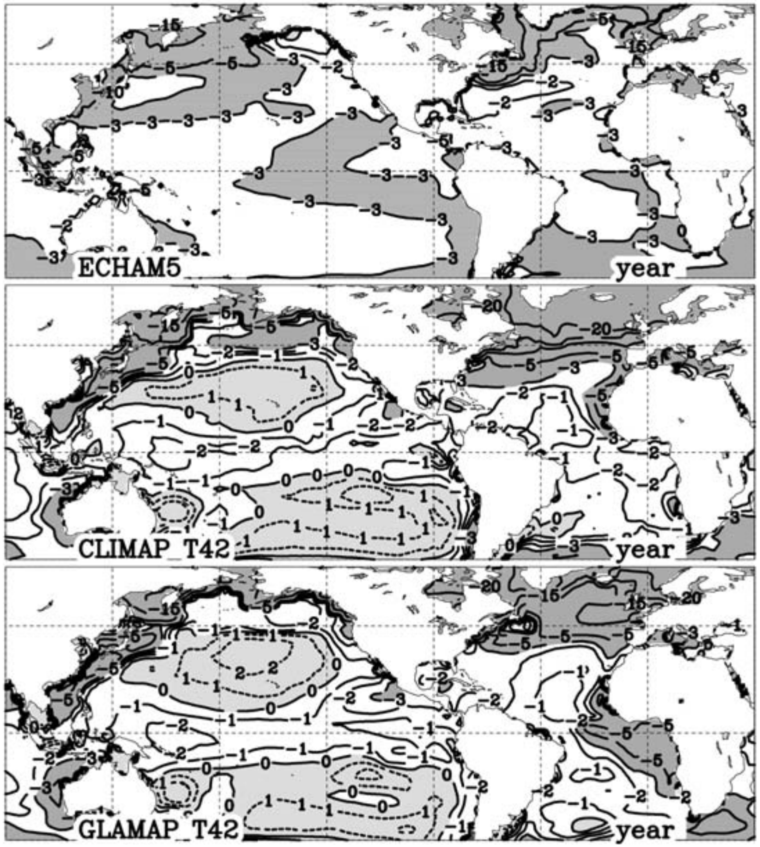

Fig. 1. Annual mean SST differences between LGM. Contours at ±0, 1, 2, 3, 5, 10, 15 °C, shading for >0 and < −3 °C. Positive contours are dashed. Data from the models used here are surface temperatures which over sea ice can become very low.

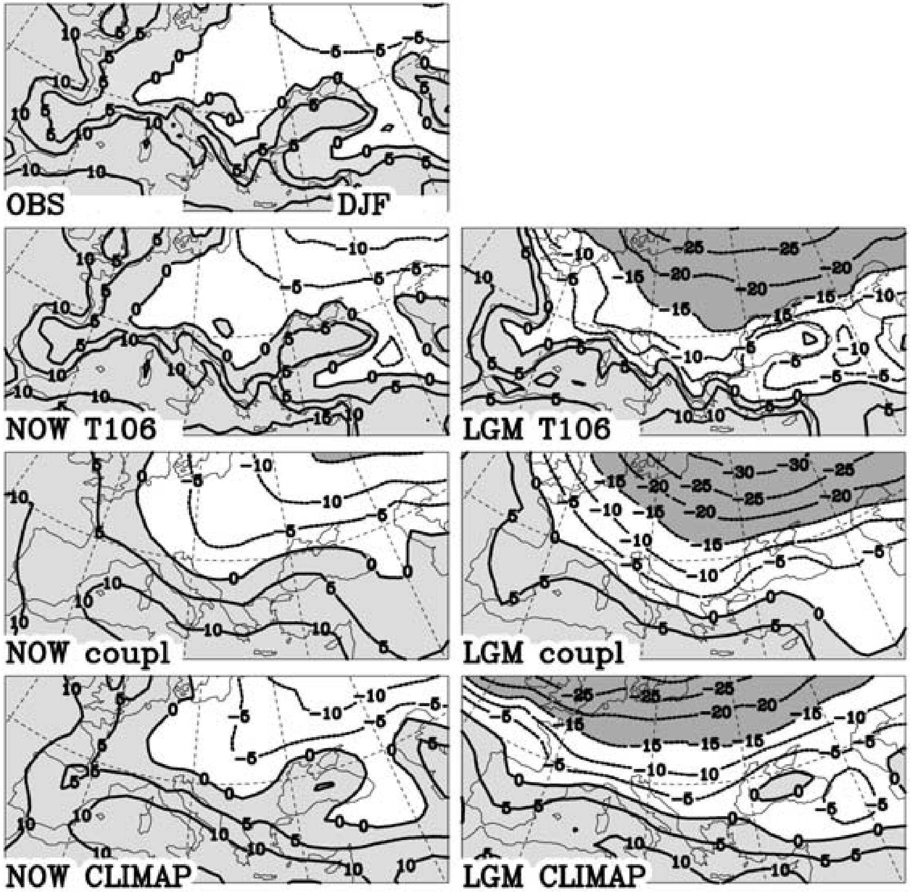

Fig. 2. 2 m temperatures for LGM and NOW as simulated, OBS is the present as analyzed by ERA40 (Uppala et al., 2005). Contours every 5 °C, down to −30 °C, **(a)** for winter, shading for >0 and < −15 °C, **(b)** for summer, shading for >20 and <10 °C.

Title Page
Abstract
Introduction
Conclusions
References
Tables
Figures
◄◄
►►
◄
►
Back
Close
Full Screen / Esc
Printer-friendly Version
Interactive Discussion

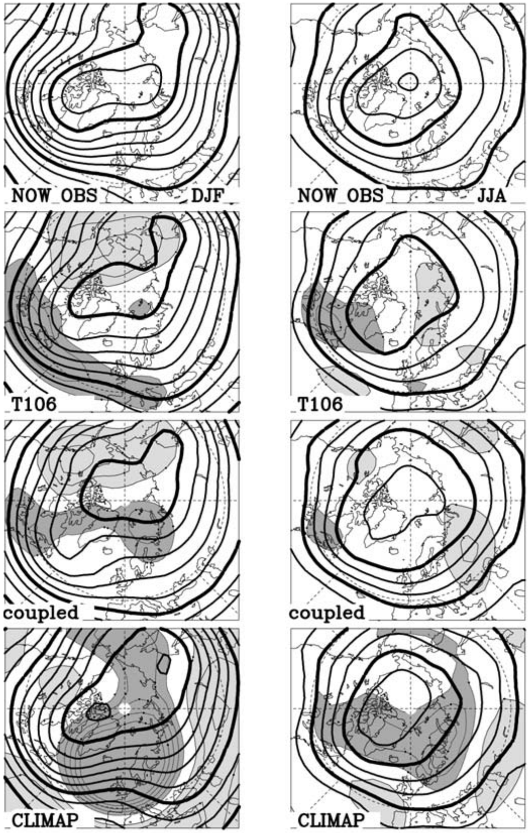

Fig. 3. 500 hPa geopotential height field for the present (heavy lines) overlaid by the difference LGM-NOW (thin lines with shading). Contours for the height field every 8 dam, highlighted lines for 516 and 556 dam in DJF (left) and for 556 and 580 dam in JJA (right). Contours for the differences at ±4, 8, 12 dam, shading for > or <4 dam, dashes and darker shading for LGM<NOW.

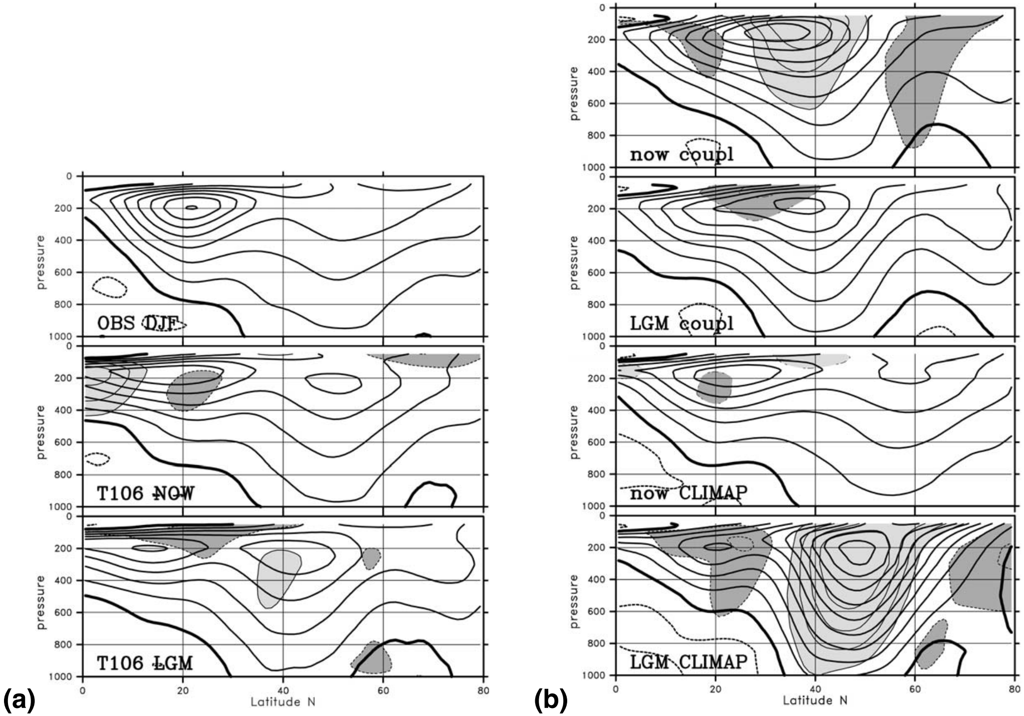

Fig. 4. Zonal wind for winter (DJF) averaged between 30° W and 10° E overlaid in thin lines with shading the difference to the observation for the present (NOW) or the difference to NOW for the LGM. Contours every 5 m s^{-1}, heavy line for the 0-zonal wind contour. Light shading for increases of zonal winds for the simulations of the present compared to the observations or for the LGM compared to the present by more than 5 m s^{-1} and dark shading (dashed contours) for decreases by more than 5 m s^{-1}. **(a)** Analysis and T106 simulation. **(b)** Coupled and CLIMAP simulation.

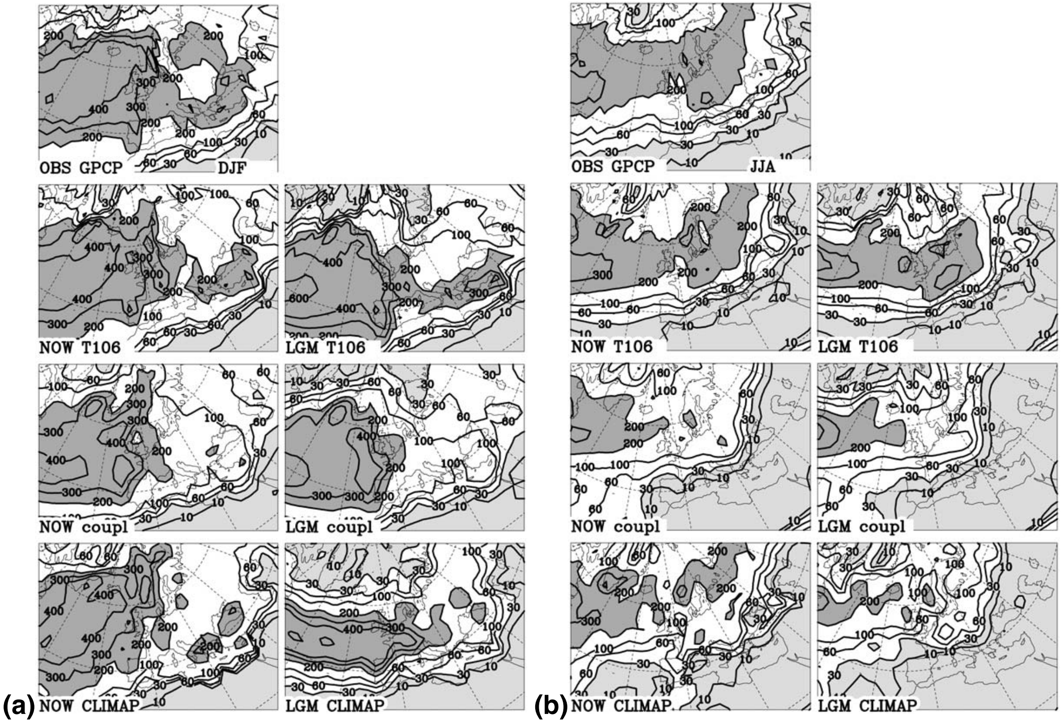

Fig. 5. Precipitation as estimated for the truth (GPCP, Huffman et al., 1996) and simulated by the models. Contours at 10, 30, 60, 100, 200, 300, 400, 600, shading for <30 and >200 mm season^{-1}, **(a)** for winter, **(b)** for summer.

Title Page
Abstract
Introduction
Conclusions
References
Tables
Figures
◀▌
▶▌
◀
▶
Back
Close
Full Screen / Esc
Printer-friendly Version
Interactive Discussion

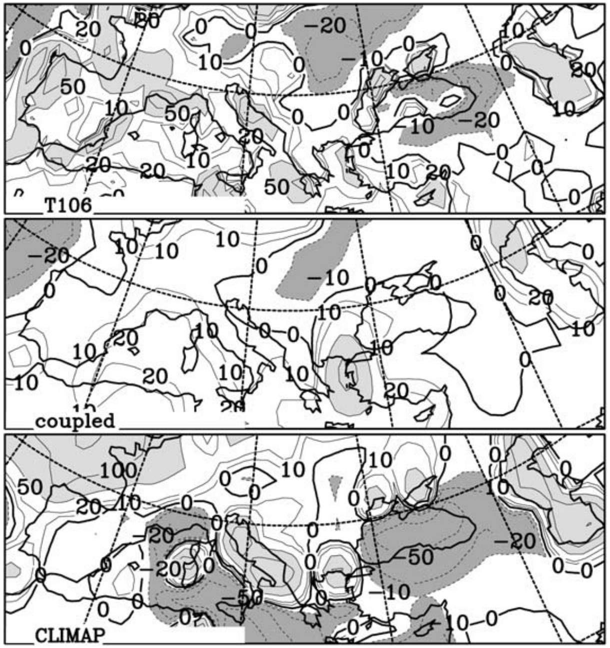

Fig. 6. Annual mean precipitation minus evaporation (P-E) in the simulations, difference between LGM and NOW. Contours at ±0, 10, 20, 50, 100, 200 mm season^{-1}, shading for >50 and < −10 mm season^{-1}. Negative contours are dashed.

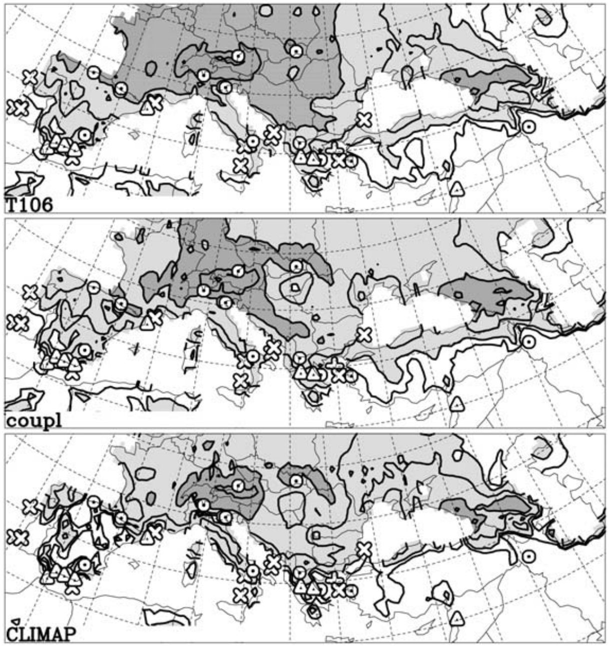

Fig. 7. Summer precipitation during LGM down-scaled to a 0.5° grid. Contours at 30, 50, 100, 200, 400 mm season^{-1}, shading for >50 and darker for >200 mm season^{-1}. Sites with observed summer-green tree growth during LGM are indicated by markers. Circles: only cold-tolerant trees (continental), triangles: cool or warm-loving trees (continental), Xs: only cold-tolerant trees (marine), crosses: cool or warm-loving trees (marine).

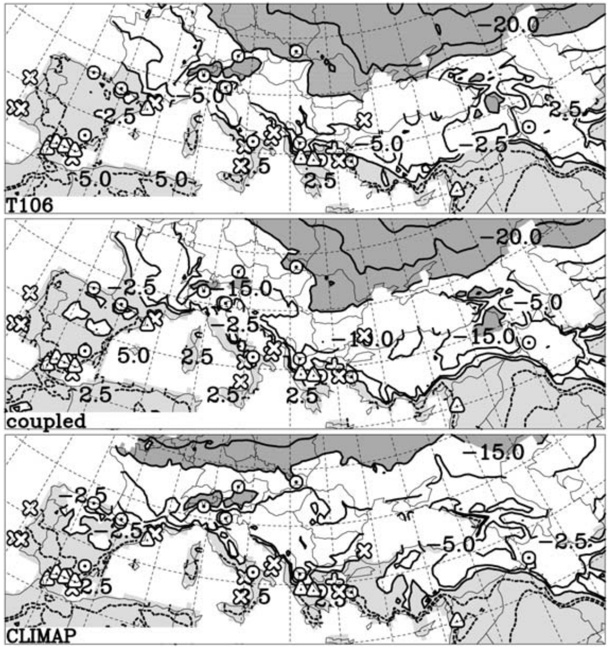

Fig. 8. 2 m temperature of the coldest month. Contours at ±2.5, 5, 10, 15, 20 °C, shading for > −2.5 and < −15 °C. Dashes for positive contours. Sites with observed summer-green tree growth during LGM are indicated by markers. Circles: only cold-tolerant trees (continental), triangles: cool or warm-loving trees (continental), Xs: only cold-tolerant trees (marine), crosses: cool or warm-loving trees (marine).

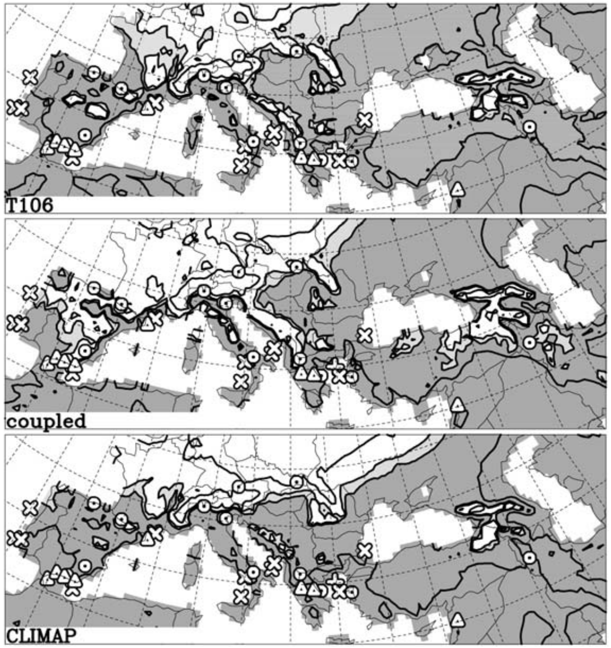

Fig. 9. Growing degree days above 5 °C. Contours at 300, 800, 1000, 2000, 5000, shading for >800 and in darker shading for >1000. Sites with observed tree growth during LGM are indicated by markers. Circles: only cold-tolerant trees (continental), triangles: cool or warm-loving trees (continental), Xs: only cold-tolerant trees (marine), crosses: cool or warm-loving trees (marine).

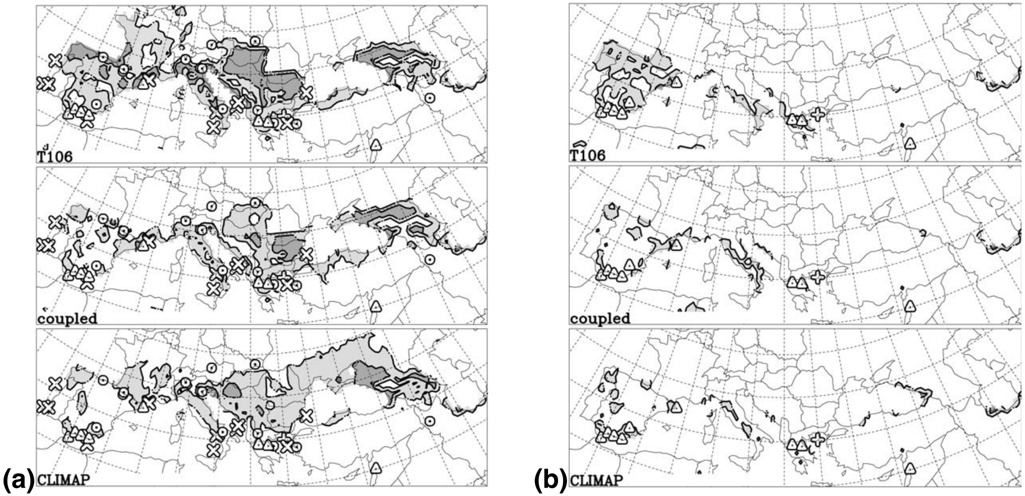

Fig. 10. Likeliness of tree growth during the LGM combining the summer precipitation, minimum temperature and growing degree days. Contours and shading for >1 and 5. Values of 1 and higher suggest possible tree growth, higher values mean higher likeliness. Sites with observed tree growth during LGM are indicated by markers. Circles: only cold-tolerant trees (continental), triangles: cool or warm-loving trees (continental), Xs: only cold-tolerant trees (marine), crosses: cool or warm-loving trees (marine). **(a)** cold-tolerant trees, **(b)** warm-loving trees.